Hindawi Publishing Corporation
Advances in Materials Science and Engineering
Volume 2014, Article ID 535640, 9 pages
http://dx.doi.org/10.1155/2014/535640

Research Article

Sintering Behavior of CNT Reinforced Al6061 and Al2124 Nanocomposites

Nouari Saheb[1,2]

[1] *Mechanical Engineering Department, King Fahd University of Petroleum & Minerals, Dhahran 31261, Saudi Arabia*
[2] *Center of Excellence in Nanotechnology, King Fahd University of Petroleum & Minerals, Dhahran 31261, Saudi Arabia*

Correspondence should be addressed to Nouari Saheb; nouari@kfupm.edu.sa

Received 27 October 2013; Revised 12 May 2014; Accepted 20 May 2014; Published 3 June 2014

Academic Editor: Rui Zhang

Ball milling and spark plasma sintering were successfully used to produce carbon nanotube reinforced Al6061 and Al2124 nanocomposites which have potential applications in the fields of aerospace, automotive, electronics, and high precision instrumentation. Al2124 and Al6061 nanocomposite powders containing 0.5 to 2 wt.% CNTs prepared through sonication and wet ball milling were spark plasma sintered at 400, 450, and 500°C for 20 minutes under a pressure of 35 MPa. CNTs were better dispersed, and less agglomerated and had good adhesion to the matrix in composites containing 1 wt.% CNTs. The increase of CNT content to 2 wt.% led to the formation of CNT clusters which resulted in less uniform and homogenous composite powders. Almost full densification of Al6061 reinforced with CNTs was achieved at 500°C. Also, CNTs reinforced Al2124 nanocomposites reached very high densities at 500°C. Composites reinforced with 1 wt.% CNTs displayed better densification compared to composites containing 2 wt.% CNTs. The increase of CNTs content from 0.5 to 1 wt.% increased the hardness of the Al6061 and Al2124 alloys to maximum values. Further increase of CNTs content to 2 wt.% decreased the hardness to values lower than that of the monolithic alloys.

1. Introduction

Spark plasma sintering (SPS) has been proven to be effective nontraditional powder metallurgy technique to sinter fully dense metallic materials in short sintering times at relatively low sintering temperatures [1, 2]. Substantial benefits can be achieved by SPS over conventional sintering. Spark plasma sintered compacts retain their fine microstructures and achieve very high density under reduced sintering temperature and time. In addition, SPS not only is a binderless process but also does not require a precompaction step. The powder is directly filled into a graphite die through which the current is passed and the resulting sample is a material with superior mechanical properties. The SPS process is being used to consolidate different types of materials [3, 4].

Recently, nanocomposite materials have received the serious attention of researchers in view of their much better properties than those of either the monolithic material or the composite containing a coarse-grained reinforcement phase [5]. However, agglomeration and poor distribution/dispersion of the reinforcement in the matrix remain a major problem in processing homogeneous metal matrix nanocomposites [6]. Solid-state processing methods such as mechanical alloying are being used to uniformly disperse high volume fraction of the reinforcement in metal matrix nanocomposites and overcome the problem of agglomeration. Mechanical alloying [7–10], also called ball milling, is a powder metallurgy processing technique which involves cold welding, fracturing, and rewelding of powder particles in a ball mill. It is used to synthesize a variety of materials including nanocomposites. It has many advantages as a processing technique which includes being simple, versatile, and economically viable and enables the synthesis of novel materials.

Carbon nanotubes (CNTs), discovered by Iijima [11] and proved exceptionally strong by Wong and coworkers [12], have been manifested as very promising nanoreinforcement for the improvement of mechanical and physical properties of various metallic materials including Al6061 and Al2124 alloys which have potential applications in the fields of aerospace, automotive, electronics, and high precision instrumentation.

However, uniform distribution of the reinforcement phase during mixing and grain growth of the matrix phase during consolidation remained major challenges in the development of CNT reinforced metal matrix nanocomposites. Although some researchers [13, 14] reported unsatisfactory improvement in the mechanical properties of aluminum as a result of CNTs addition, others reported dramatic improvement in these properties [15–22]. The change of mechanical properties was found to be sensitive to CNTs content and sintering temperature [23–27].

In previous works, we reported the effect of ball milling on the dispersion of CNTs in Al-nanocomposites [28] and investigated the effect of sintering parameters on the densification and hardness of Al6061 and Al2124 aluminum alloys [2, 29, 30]. The objective of the present work is to investigate the sintering behavior of carbon nanotube reinforced Al2124 and Al6061 nanocomposites prepared through spark plasma sintering. The microstructure, hardness, and density of sintered samples will be characterized and evaluated as function of CNT content and sintering temperature.

2. Materials and Experimental Procedures

The Al6061 and Al2124 prealloyed powders used in this study were supplied by the Aluminium Powder CO. LTD. The chemical composition of the powders presented in Table 1 was determined by X-ray fluorescence (XRF) using a spectrometer machine with Rh tube, operated at a voltage of 30 kV and a current of 1.020 mA. CNTs having an average diameter of 24 nm and a length of a few microns were produced by the floating catalyst chemical vapor deposition (FC-CVD) method. Al2124 and Al6061 nanocomposite powders containing 0.5, 0.75, 1, and 2 wt.% CNTs were prepared through wet ball milling using a Fritsch P5 planetary ball mill. CNTs were put into water (1 : 500 ratio) and were sonicated in a probe sonicator for 30 minutes; a 50% power sonication was used. The prealloyed powder was added followed by sonication of the mixture for 15 minutes. The sonicated slurry was charged into cylindrical stainless steel vials (250 mL in volume) together with stainless steel balls (10 mm in diameter) and wet-milled for 1 hour. The wet milling experiments were carried out at room temperature at a speed of 200 rpm in argon atmosphere to prevent the oxidation of the powders. A ball to powder weight ratio of 10 : 1 was used. Fully automated (FCT system, Germany) spark plasma sintering equipment model HP D 5 was used to sinter the samples. The dried nanocomposite powders were directly charged into graphite die through which the current is passed. A 20 mm graphite die was used and a pressure of 35 MPa was applied during the whole sintering process, that is, during heating and holding time. The heating rate was 100 K/min. The samples were vacuum-sintered at 400, 450, and 500°C for 20 minutes. The sintering temperature was measured using a thermocouple inserted in the graphite die through a drilled hole. A graphite sheet was used to minimize friction between die walls and the powder as well as to ease the ejection of samples after sintering. A JEOL scanning electron microscope (SEM) model JSM 6460 was used to characterize the raw powders and analyze the microstructure of sintered samples. Field-emission dual beam scanning electron microscope that combines a high-end field-emission scanning electron microscope (FESEM) and a high-performance focused ion beam (FIB) system in one chamber (model Tescan Lyra-3) was used to characterize fractured surfaces of sintered samples. The density of sintered samples was measured using Alfa Mirage electronic densimeter (model MD-300s) and quantified according to Archimedes principle. Vickers microhardness of the spark plasma sintered samples was measured using a digital microhardness tester. All measurements were conducted by applying the same conditions: load of 100 gf and time of 12 s and the data reported were the average of 10 values.

Table 1: Composition of Al2124 and Al6061 powders.

Powder	Al	Fe	Si	Cu	Mn	Mg	Zn
Al2124	93.95	0.064	0.058	3.88	0.58	1.42	0.034
Al6061	97.83	0.192	0.69	0.29	0.016	0.83	0.012

3. Results and Discussion

The morphology of Al6061 and Al2124 powders is shown in Figure 1. It can be clearly seen that the powders are composed of particles with various sizes and shapes. Figure 2 shows the morphology of CNTs produced by the floating catalyst chemical vapor deposition (FC-CVD) method. These CNTs have an average diameter of 24 nm and a length of a few microns. Typical SEM micrographs of Al6061 composite powders containing 1 and 2 wt.% CNTs are presented in Figure 3. The CNTs were better dispersed and less agglomerated and had good adhesion to the matrix in the composite containing 1 wt.% CNTs as can be seen in Figure 3(a). The increase of CNTs content to 2 wt.% led to the formation of CNT clusters, Figure 3(b), which resulted in less uniform and homogenous composite powder. Similar trend was observed with CNT reinforced Al2124 composite powder. It is well known that CNT clustering [14, 17, 23–27] hinders proper neck growth between adjacent matrix particles during sintering and results in poor densification and properties of the material. Also, it is one of the sources of considerable discrepancy between the theoretically predicted and experimentally observed mechanical properties of the composite [20]. Researchers have also reported the formation of aluminum carbide [24, 25] in case of higher CNTs percentage which is another source of weakness. The problem of aluminum carbide formation can be avoided through proper control of processing parameters such as temperature or by applying suitable coating on CNTs. Uniform dispersion of CNTs requires careful design of dispersion techniques and routes to enable maximum benefits from these extremely strong reinforcements. In the present work, a combination of sonication and wet milling was utilized to improve CNT dispersion which resulted in homogenous and uniform distribution of CNTs in composite reinforced with 1 wt.% CNTs. However, considerable agglomeration was observed in

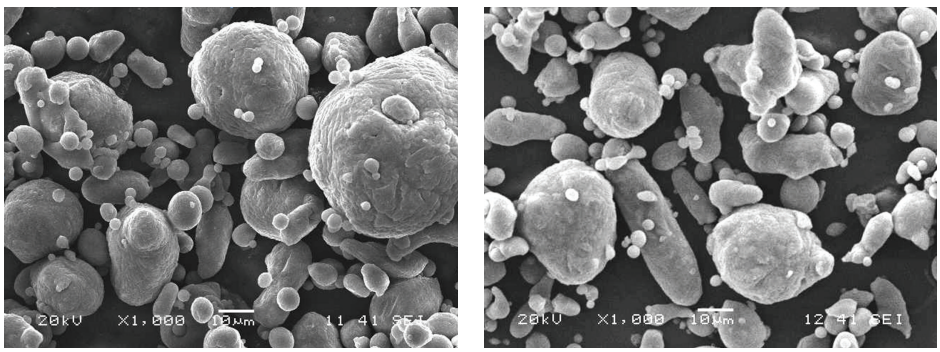

(a) (b)

Figure 1: SEM micrographs of powders: (a) Al6061 and (b) Al2124.

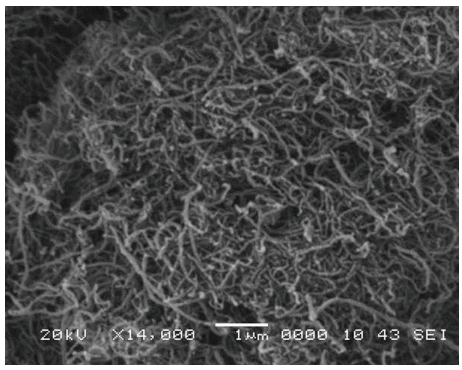

Figure 2: SEM micrographs of carbon nanotubes.

the composite containing 2 wt.% CNTs which caused poor densification and hardness of the composites as discussed below.

Figure 4 shows SEM micrographs of CNTS reinforced Al6061 nanocomposites spark plasma sintered for 20 minutes at 400, 450, and 500°C under an applied pressure of 35 MPa. Figure 4(a) shows a uniform distribution of remaining small pores after sintering Al6061 + 1 wt.% CNTs sample at 400°C. Increasing sintering temperature to 450°C promoted densification and reduced pores number and size as can be clearly seen in Figure 4(b). Almost complete densification of this material was achieved at 500°C as shown in Figure 4(c) where only very few tiny pores are present. The Al6061 + 2 wt.% CNTs nanocomposite showed similar behavior with the one reinforced with 1 wt.% CNTs. Figure 4(d) shows a uniform distribution of remaining pores after sintering Al6061 + 2 wt.% CNTs sample at 400°C. Increasing sintering temperature to 450°C promoted densification and reduced pore number and size as can be clearly seen in Figure 4(e). Complete densification of this material was achieved at 500°C as shown in Figure 4(f) and confirmed by relative density values presented below. However, Figure 4(f) shows traces of delamination (not ordinary pores) indicated by arrows. This delamination is believed to be due to grinding and polishing of samples. It is clear that at constant sintering time (20 minutes) the sintering temperature had an important influence on the densification of CNTs reinforced Al6061 nanocomposites; a similar trend was seen in the sintering of Al6061 monolithic alloy. This is because sintering is a thermally activated process controlled mainly by diffusion [31, 32]. Therefore, the higher the sintering temperature, the higher the diffusion rate and the higher the rate of pores elimination. Also, it is well known that, in spark plasma sintering, the DC pulse discharge could generate spark plasma, spark impact pressure, Joule heating, and an electrical field diffusion effect [1, 6, 33, 34]. The formation of plasma during SPS has a direct effect on sintering of particles; however, the role of current and its pulsing is still under controversy [1, 35]. Spark discharge appears in the gap between the particles of the powder where a local high temperature state of several to ten thousand °C momentarily occurs. This causes vaporization and the melting of the surfaces of the powder particles during the SPS process which dramatically enhances the rate of diffusion resulting in a sintered compact of high density.

SEM micrographs of fractured surfaces of Al6061 containing 1 wt.% CNTs are shown in Figure 5(a) at low magnification and in Figure 5(b) at high magnification. The morphology of fractured surfaces of the Al6061 containing 2 wt.% CNTs is presented in Figures 5(c) and 5(d). No clustering of CNTs was evident in the composite containing 1 wt.% CNTs. Pullout of CNTs from the matrix (indicated by arrow) due to fracture was noticed. However, clustering and poor dispersion of CNTs were clearly noticed in composite containing 2 wt.% CNTs as can be seen in Figures 5(c) and 5(d). Figure 6 shows SEM micrographs of CNTS reinforced Al2124 nanocomposites spark plasma sintered for 20 minutes at 400, 450, and 500°C under an applied pressure of 35 MPa. Good densification was achieved and not many pores are left after sintering Al2124 + 1 wt.% CNTs sample at 400°C as shown in Figure 6(a). Increasing sintering temperature to 450°C and 500°C slightly promoted densification as shown in Figures 6(b) and 6(c), respectively, and confirmed by relative density values presented below. Al2124 + 2 wt.% CNTs nanocomposite showed less densification compared with the one reinforced with 1 wt.% CNTs. Figure 6(d) shows a uniform distribution of remaining pores after sintering Al2124 + 2 wt.% CNTs sample at 400°C. The increase of sintering temperature to 450°C and 500°C improved densification as shown in Figures 6(e) and 6(f), respectively.

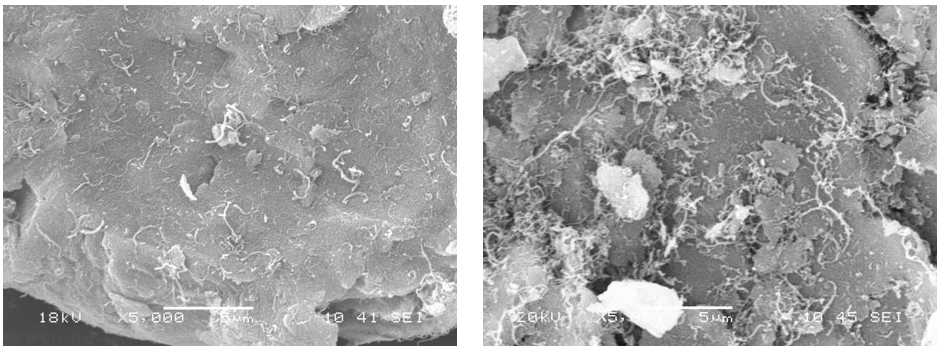

(a) (b)

Figure 3: SEM micrographs of Al6061 composite powders containing (a) 1 wt.% and (b) 2 wt.% CNTs.

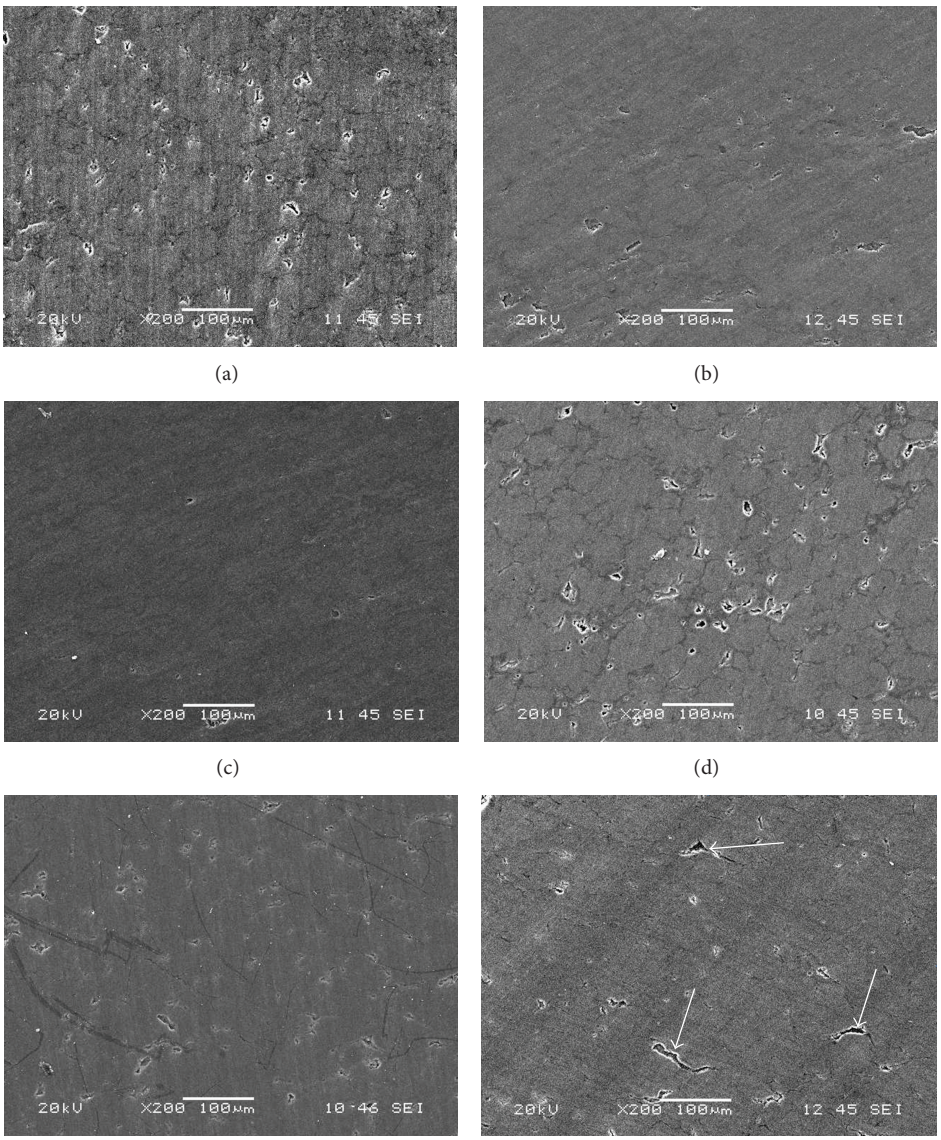

(a) (b)

(c) (d)

(e) (f)

Figure 4: SEM micrographs of Al6061 + 1 wt.% CNTs spark plasma sintered at (a) 400°C, (b) 450°C, and (c) 500°C and Al6061 + 2 wt.% CNTs spark plasma sintered at (d) 400°C, (e) 450°C, and (f) 500°C.

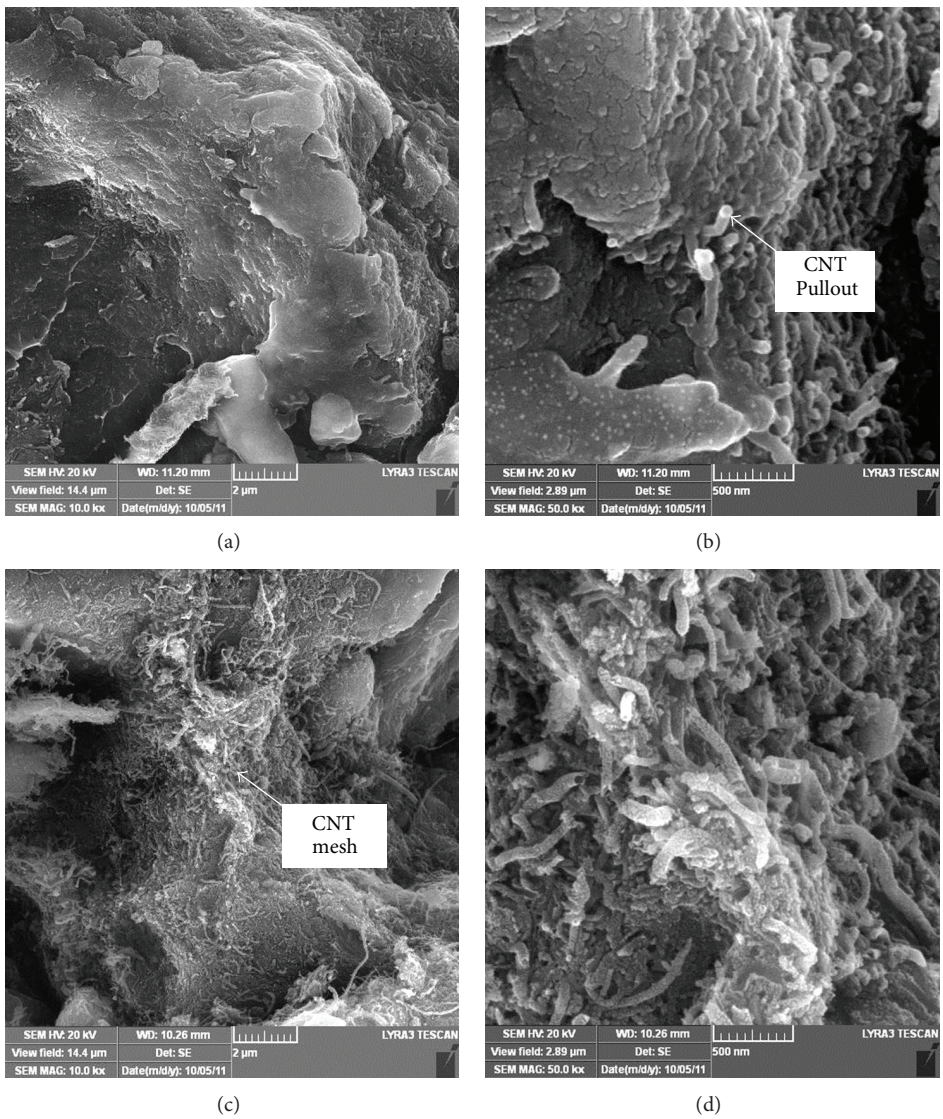

(a) (b)

(c) (d)

Figure 5: SEM micrographs of fractured surfaces of Al6061 containing (a, b) 1 wt.% CNTs and (c, d) 2 wt.% CNTs.

However, complete densification of CNTs reinforced Al2124 nanocomposites; that is, 100% was not possible at 500°C.

The density of spark plasma sintered CNT reinforced Al6061 nanocomposites as function of CNT content and sintering temperature is presented in Figure 7. A relative density of 94.07% was achieved at a sintering temperature of 400°C for the Al6061 alloy and full density; that is, 100% was obtained at 450°C. For the Al6061 + 0.5 wt.% CNTs composite, a relative density of 95.31% was achieved at a sintering temperature of 400°C; increasing sintering temperature to 450°C increased the relative density to 97.24%. A further increase of sintering temperature to 500°C increased it to 100%. A relative density of 94.55% was achieved at a sintering temperature of 400°C for the Al6061 + 0.75 wt.% CNTs composite; increasing sintering temperature to 450°C increased the relative density to 97.16%. A further increase of sintering temperature to 500°C increased it to 100%. A relative density of 95.66% was achieved at a sintering temperature of 400°C for the Al6061 + 1 wt.% CNTs composite; increasing sintering temperature to 450°C increased the relative density to 97.68%. A further increase of sintering temperature to 500°C increased it to 99.21%. Full densification of this composite, that is, relative density of 100%, was not possible at a sintering temperature of 500°C. For the Al6061 + 2 wt.% CNTs composite, a relative density of 97.77% was achieved at a sintering temperature of 400°C; increasing sintering temperature to 450°C decreased the relative density to 97.35%. However, a further increase of sintering temperature to 500°C increased it to 100% and full densification was obtained at this temperature.

The density of spark plasma sintered CNT reinforced Al2124 nanocomposites as function of CNT content and sintering temperature is presented in Figure 8. A relative density of 93.48% was achieved for the Al2124 alloy sintered at 400°C. Increasing the sintering temperature to 450°C increased the relative density to 99.17%. Almost full

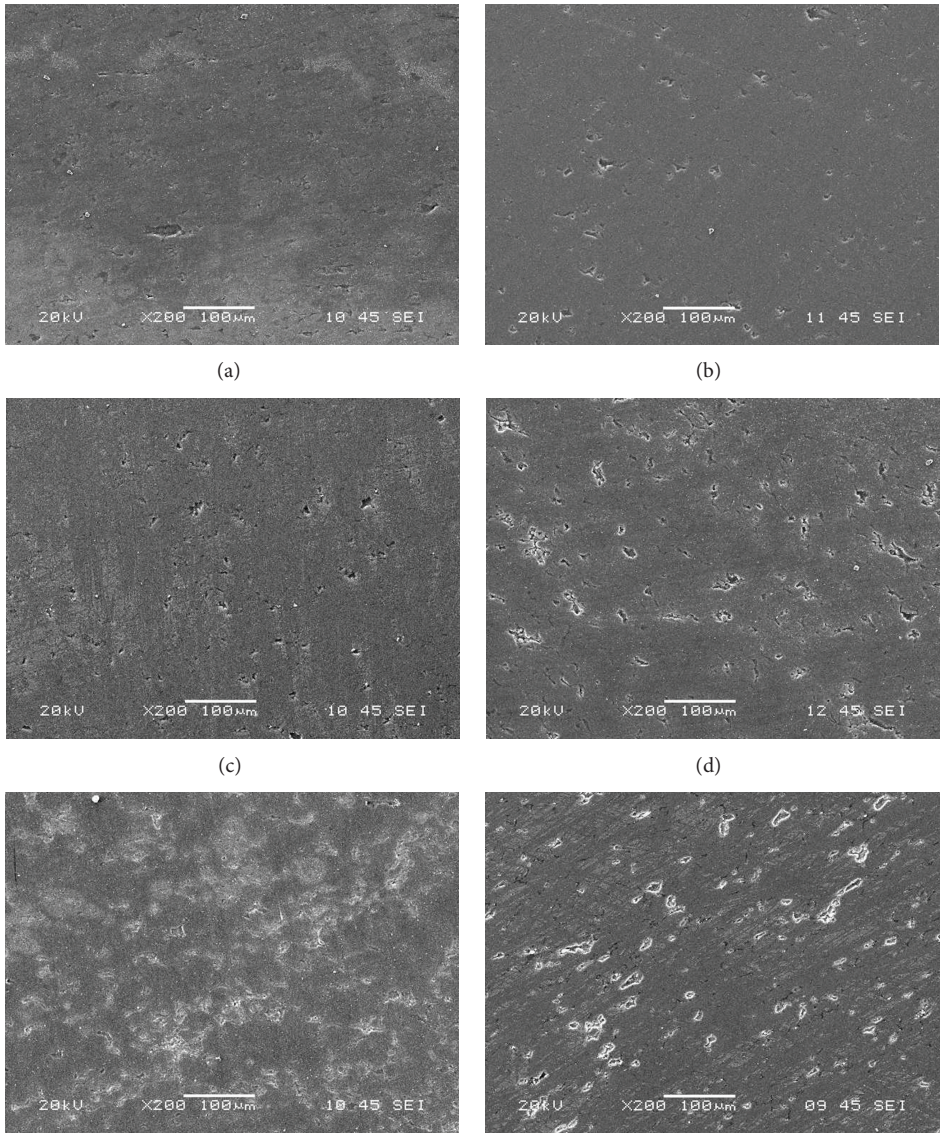

Figure 6: SEM micrographs of Al2124 + 1 wt.% CNTs spark plasma sintered at (a) 400°C, (b) 450°C, and (c) 500°C and Al2124 + 2 wt.% CNTs spark plasma sintered at (d) 400°C, (e) 450°C, and (f) 500°C.

densification of this alloy, that is, relative density of 99.64%, was possible at a sintering temperature of 500°C. For the Al2124 + 0.5 wt.% CNTs composite, a relative density of 96.56% was achieved at a sintering temperature of 400°C; increasing sintering temperature to 450°C increased the relative density to 98.62%. A further increase of sintering temperature to 500°C increased the density to 99.56%. A relative density of 96.66% for the Al2124 + 0.75 wt.% CNTs composite was achieved at a sintering temperature of 400°C; increasing sintering temperature to 450°C increased the relative density to 99.13%. A further increase of sintering temperature to 500°C increased the density to 99.67%. A relative density of 96.14% was obtained at a sintering temperature of 400°C for the Al2124 + 1 wt.% CNTs composite; increasing sintering temperature to 450°C increased the relative density to 98.36%. A further increase of sintering temperature to 500°C had only very small effect and increased the density to 98.40%. For the Al2124 + 2 wt.% CNTs composite, a relative density of 94.13% was achieved at a sintering temperature of 400°C; increasing sintering temperature to 450°C increased the relative density to 95.92%. A further increase of sintering temperature to 500°C increased the density to 97.79%. In CNTs reinforced composites, samples containing 1 wt.% CNTs displayed better densification compared with samples containing 2 wt.% CNTs. The sintered composites displayed good densification and high relative densities. This is due to the fact that field assisted consolidation methods such as spark plasma sintering are capable of providing high instantaneous energy for sintering nanocomposites [19, 21, 24, 26] compared to conventional sintering methods

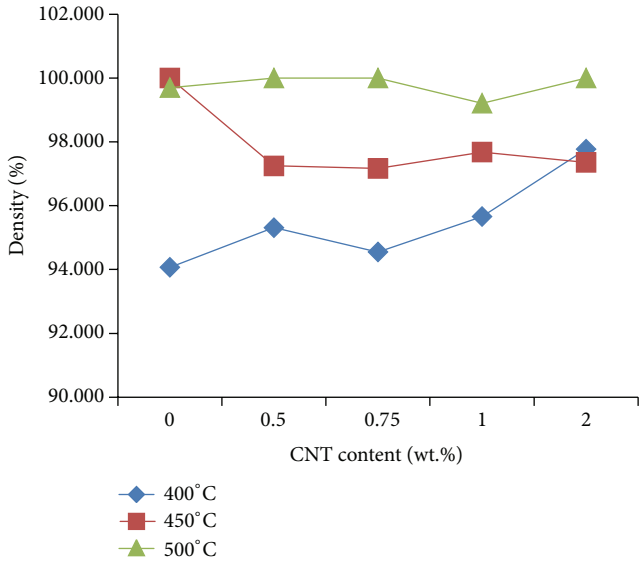

Figure 7: Relative density of CNT reinforced Al6061 nanocomposites.

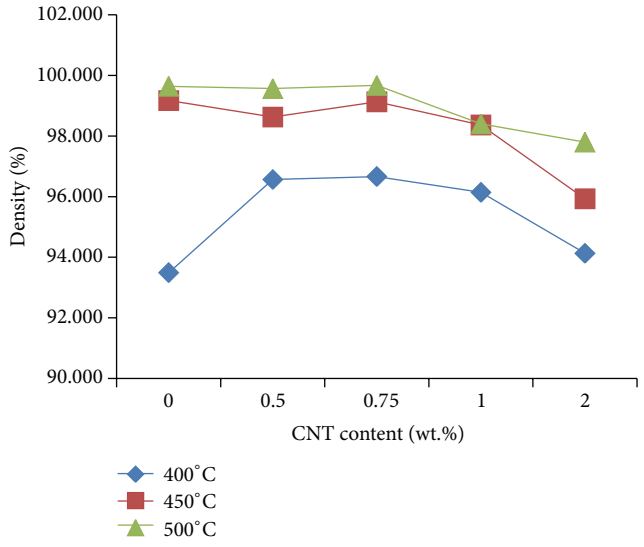

Figure 8: Relative density of CNT reinforced Al2124 nanocomposites.

such as hot pressing [13] and furnace sintering [15] which are not capable of properly densifying nanocomposites as these methods provide less instantaneous interfacial energy between particles for bonding.

Vickers microhardness of spark plasma sintered CNT reinforced Al6061 nanocomposites as function of CNT content and sintering temperature is presented in Figure 9. Increasing sintering temperature from 400 to 450°C for the Al6061 + 0.5 wt.% composite increased the microhardness from 59.19 to 67.02. A further increase of sintering temperature to 500°C decreased it to 66.48. For the Al6061 + 0.75 wt.% composite, increasing sintering temperature from 400 to 450°C increased the microhardness from 59.95 to 67.7. A further increase of sintering temperature to 500°C decreased

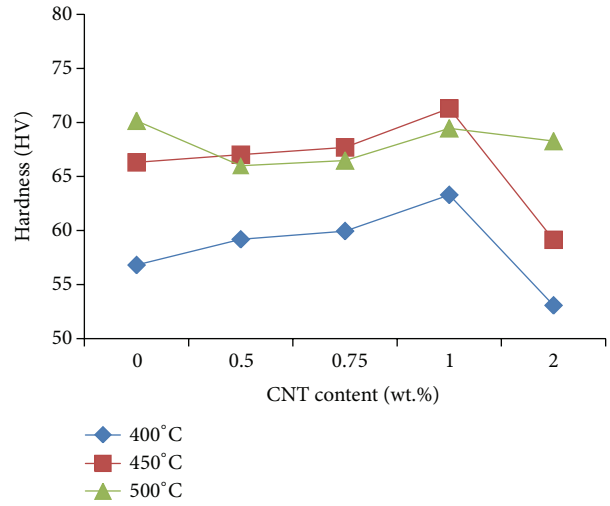

Figure 9: Microhardness of CNT reinforced Al6061 nanocomposites.

it to 66.48. For the Al6061 + 1 wt.% composite, increasing sintering temperature from 400 to 450°C increased the microhardness from 63.30 to 71.30. A further increase of sintering temperature to 500°C decreased it to 69.46. For the Al6061 + 2 wt.% composite, the increase of sintering temperature from 400 to 450°C increased the microhardness from 53.08 to 59.15. A further increase of sintering temperature to 500°C increased the microhardness to 68.28. The change of microhardness with sintering temperature matched the change of relative density as a function of sintering temperature; this is due to the fact that both relative density and microhardness depend on the amount of pores in the material. The increase of CNT content up to 1 wt.% increased the microhardness of Al6061 samples sintered at 400°C and 450°C. A further increase of CNT content to 2 wt.% led to the decrease of the microhardness to values lower than the value of Al6061 monolithic alloy. However, at a sintering temperature of 500°C the increase of CNT content did not improve the microhardness of samples. Vickers microhardness of spark plasma sintered CNT reinforced Al2124 nanocomposites as function of CNT content and sintering temperature is presented in Figure 10. Increasing sintering temperature from 400 to 450°C for the Al2124 + 0.5 wt.% composite increased the microhardness from 87.7 to 118.88. A further increase of sintering temperature to 500°C decreased it to 117.25. For the Al2124 + 0.75 wt.% composite, increasing sintering temperature from 400 to 450°C increased the microhardness from 88.82 to 119.42. A further increase of sintering temperature to 500°C increased it to 120.33. For the Al2124 + 1 wt.% composite, increasing sintering temperature from 400 to 450°C increased the microhardness from 102.55 to 120.87. A further increase of sintering temperature to 500°C decreased it to 121.67. For the Al2124 + 2 wt.% composite, the increase of sintering temperature from 400 to 450°C increased the microhardness from 83.64 to 105.5. A further increase of sintering temperature to 500°C decreased it to 103.77. The change of microhardness with sintering temperature almost matched the change of relative density as a function of

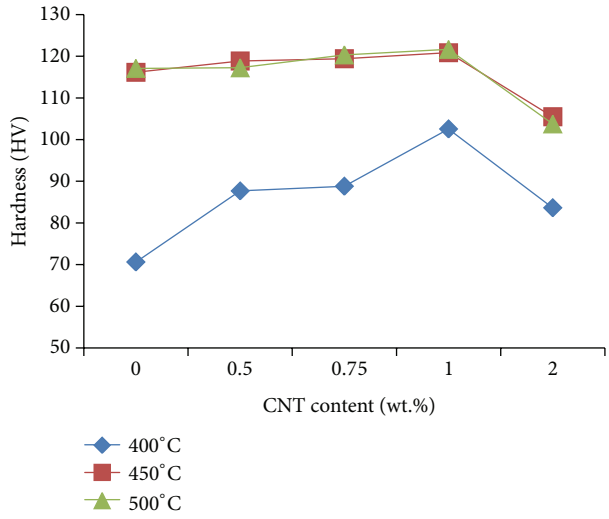

Figure 10: Microhardness of CNT reinforced Al2124 nanocomposites.

sintering temperature. The increase of CNT content up to 1 wt.% in Al2124 samples sintered at 400, 450, and 500°C increased the microhardness. A further increase of CNT content to 2 wt.% led to the decrease of the microhardness of samples. Al2124 reinforced with 2 wt.% CNT displaced lower hardness compared to unreinforced samples; the same trend was observed in Al6061 based composites. The above results show that the addition of up to 1 wt.% CNTs improved the hardness of the composites, but CNT content higher than 1 wt.% decreased it. These results are in agreement with those published in the literature. Esawi and Elborady [23] reported enhancement in mechanical properties upon addition of lower proportion of CNTs, but for higher CNT contents, opposite trend was observed which was attributed to the presence of CNT clusters. Similar trend was observed by Kim and coworkers [24] who found highest hardness and wear resistance for Al in case of 1 wt.% CNTs and for higher CNT content poor characteristics were attributed to CNT agglomeration and formation of aluminum carbide. Also, maximum tensile and compressive properties were reported [26] for 0.5 wt.% CNTs and decreasing trend was observed for much higher CNT percentages.

4. Conclusion

Carbon nanotube reinforced Al6061 and Al2124 nanocomposites were prepared through sonication followed by wet ball milling and consolidated through spark plasma sintering. CNTs were better dispersed and less agglomerated and had good adhesion to the matrix in composites containing 1 wt.% CNTs. The increase of CNT content to 2 wt.% led to the formation of CNT clusters which resulted in less uniform and homogenous composite powders. Almost full densification of Al6061 reinforced with CNTs was achieved at 500°C. Also, CNTs reinforced Al2124 nanocomposites reached very high densities at 500°C. Composites reinforced with 1 wt.% CNTs displayed better densification compared to composites containing 2 wt.% CNTs. The increase of CNTs content from 0.5 to 1 wt.% increased the hardness of the Al6061 and Al2124 alloys to maximum values. Further increase of CNTs content to 2 wt.% decreased the hardness to values lower than that of the monolithic alloys.

Conflict of Interests

The author declares that there is no conflict of interests regarding the publication of this paper.

Acknowledgment

The author would like to acknowledge financial support from King Abdul Aziz City for Science and Technology (KACST) through research Project no. ARP-28-122.

References

[1] N. Saheb, Z. Iqbal, A. Khalil et al., "Spark plasma sintering of metals and metal matrix nanocomposites: a review," *Journal of Nanomaterials*, vol. 2012, Article ID 983470, 13 pages, 2012.

[2] N. Saheb, "Spark plasma and microwave sintering of Al6061 and Al2124 alloys," *International Journal of Minerals, Metallurgy and Materials*, vol. 20, no. 2, pp. 152–159, 2013.

[3] L. W. Lu and W. G. Qin, *Archives of Metallurgy and Materials*, vol. 56, no. 4, pp. 1271–1276, 2011.

[4] O. Petukhov, I. Khobta, A. Ragulya, and Y. Sakka, "Synthesis of the TiN-TiB_2 ceramic composites under various spark plasma sintering conditions," *Archives of Metallurgy and Materials*, vol. 54, no. 4, pp. 957–962, 2009.

[5] C. Suryanarayana, "Synthesis of nanocomposites by mechanical alloying," *Journal of Alloys and Compounds*, vol. 509, supplement 1, pp. S229–S234, 2011.

[6] V. Viswanathan, T. Laha, K. Balani, A. Agarwal, and S. Seal, "Challenges and advances in nanocomposite processing techniques," *Materials Science and Engineering R*, vol. 54, no. 5-6, pp. 121–285, 2006.

[7] C. Suryanarayana, "Mechanical alloying and milling," *Progress in Materials Science*, vol. 46, no. 1-2, pp. 1–184, 2001.

[8] J. Sidor, *Archives of Metallurgy and Materials*, vol. 52, no. 3, pp. 407–414, 2007.

[9] M. Chmielewski, D. Kaliński, K. Pietrzak, and W. Włosiński, "Relationship between mixing conditions and properties of sintered 20AlN/80Cu composite materials," *Archives of Metallurgy and Materials*, vol. 55, no. 2, pp. 579–585, 2010.

[10] T. Pawlik, M. Sopicka-Lizer, D. Michalik, and T. Wtodek, "Characterization of the mechanochemically processed silicon nitride-based powders," *Archives of Metallurgy and Materials*, vol. 56, no. 4, pp. 1205–1210, 2011.

[11] S. Iijima, "Helical microtubules of graphitic carbon," *Nature*, vol. 354, no. 6348, pp. 56–58, 1991.

[12] E. W. Wong, P. E. Sheehan, and C. M. Liebert, "Nanobeam mechanics: elasticity, strength, and toughness of nanorods and nanotubes," *Science*, vol. 277, no. 5334, pp. 1971–1975, 1997.

[13] T. Kuzumaki, K. Miyazawa, H. Ichinose, and K. Ito, "Processing of carbon nanotube reinforced aluminum composite," *Journal of Materials Research*, vol. 13, no. 9, pp. 2445–2449, 1998.

[14] W. Salas, N. G. Alba-Baena, and L. E. Murr, "Explosive shock-wave consolidation of aluminum powder/carbon nanotube

aggregate mixtures: optical and electron metallography," *Metallurgical and Materials Transactions A: Physical Metallurgy and Materials Science*, vol. 38, no. 12, pp. 2928–2935, 2007.

[15] T. Noguchi, A. Magario, S. Fukazawa, S. Shimizu, J. Beppu, and M. Seki, "Carbon nanotube/aluminium composites with uniform dispersion," *Materials Transactions*, vol. 45, no. 2, pp. 602–604, 2004.

[16] C. Deng, X. Zhang, D. Wang, Q. Lin, and A. Li, "Preparation and characterization of carbon nanotubes/aluminum matrix composites," *Materials Letters*, vol. 61, no. 8-9, pp. 1725–1728, 2007.

[17] C. Deng, D. Wang, X. Zhang, and A. Li, "Processing and properties of carbon nanotubes reinforced aluminum composites," *Materials Science and Engineering: A*, vol. 444, no. 1-2, pp. 138–145, 2007.

[18] S.-M. Zhou, X.-B. Zhang, Z.-P. Ding, C.-Y. Min, G.-L. Xu, and W.-M. Zhu, "Fabrication and tribological properties of carbon nanotubes reinforced Al composites prepared by pressureless infiltration technique," *Composites Part A: Applied Science and Manufacturing*, vol. 38, no. 2, pp. 301–306, 2007.

[19] K. Morsi, A. M. K. Esawi, P. Borah, S. Lanka, and A. Sayed, "Characterization and spark plasma sintering of mechanically milled aluminum-carbon nanotube (CNT) composite powders," *Journal of Composite Materials*, vol. 44, no. 16, pp. 1991–2003, 2010.

[20] T. Laha, Y. Chen, D. Lahiri, and A. Agarwal, "Tensile properties of carbon nanotube reinforced aluminum nanocomposite fabricated by plasma spray forming," *Composites Part A: Applied Science and Manufacturing*, vol. 40, no. 5, pp. 589–594, 2009.

[21] H. Kwon, D. Hoon, J. François, and A. Kawasaki, "Investigation of carbon nanotube reinforced aluminum matrix composite materials," *Composites Science and Technology*, vol. 70, no. 3, pp. 546–550, 2010.

[22] Y. Wu and G. Y. Kim, "Carbon nanotube reinforced aluminum composite fabricated by semi-solid powder processing," *Journal of Materials Processing Technology*, vol. 211, no. 8, pp. 1341–1347, 2011.

[23] A. Esawi and M. Elborady, "Carbon nanotube-reinforced aluminium strips," *Composites Science and Technology*, vol. 68, no. 2, pp. 486–492, 2008.

[24] I.-Y. Kim, J.-H. Lee, G.-S. Lee, S.-H. Baik, Y.-J. Kim, and Y.-Z. Lee, "Friction and wear characteristics of the carbon nanotube-aluminum composites with different manufacturing conditions," *Wear*, vol. 267, no. 1–4, pp. 593–598, 2009.

[25] A. M. K. Esawi, K. Morsi, A. Sayed, M. Taher, and S. Lanka, "Effect of carbon nanotube (CNT) content on the mechanical properties of CNT-reinforced aluminium composites," *Composites Science and Technology*, vol. 70, no. 16, pp. 2237–2241, 2010.

[26] J.-Z. Liao, M.-J. Tan, and I. Sridhar, "Spark plasma sintered multi-wall carbon nanotube reinforced aluminum matrix composites," *Materials and Design*, vol. 31, no. 1, pp. S96–S100, 2010.

[27] H. J. Choi, S. M. Lee, and D. H. Bae, "Wear characteristic of aluminum-based composites containing multi-walled carbon nanotubes," *Wear*, vol. 270, no. 1-2, pp. 12–18, 2010.

[28] N. Saheb, "Effect of processing on the dispersion of CNTs in al-nanocomposites," *Advanced Materials Research*, vol. 239–242, pp. 759–763, 2011.

[29] N. Saheb, "Spark Plasma Sintering of Al6061 and Al2124 Alloys," *Advanced Materials Research*, vol. 284–286, pp. 1656–1660, 2011.

[30] A. Khalil, A. S. Hakeem, and N. Saheb, "Optimization of process parameters in spark plasma sintering Al6061 and Al2124 aluminum alloys," *Advanced Materials Research*, vol. 328–330, pp. 1517–1522, 2011.

[31] R. M. German, "Scientific status of metal powder injection molding," *International Journal of Powder Metallurgy*, vol. 36, no. 3, pp. 31–36, 2000.

[32] R. M. German, *Sintering Theory and Practice*, John Wiley, New York, NY, USA, 1996.

[33] J. Adachi, K. Kurosaki, M. Uno, and S. Yamanaka, "Porosity influence on the mechanical properties of polycrystalline zirconium nitride ceramics," *Journal of Nuclear Materials*, vol. 358, no. 2-3, pp. 106–110, 2006.

[34] X. Jin, L. Gao, and J. Sun, "Preparation of nanostructured Cr1-xTixN ceramics by spark plasma sintering and their properties," *Acta Materialia*, vol. 54, no. 15, pp. 4035–4041, 2006.

[35] Y.-H. Kim, T. Sekino, T. Kusunose, T. Nakayama, K. Niihara, and H. Kawaoka, "Electrical and mechanical properties of K, Ca ionic-conductive silicon nitride ceramics," *Ceramic Transactions*, vol. 165, pp. 31–38, 2005.